

Supporting Information

From the Synthesis to the Device: Elucidating Structural and Electronic Properties of C7-BTBT-C7

Priya Pandey^{‡†}, Lamiaa Fijahi[‡], Nemo McIntosh[§], Nicholas Turetta[¥], Marco Bardini[§], Samuele Giannini[§], Christian Ruzié[¤], Guillaume Schweicher[¤], David Beljonne[§], Jérôme Cornil[§], Paolo Samori[¥], Marta Mas-Torrent^{‡*}, Yves Henri Geerts^{¤¤*}, Enrico Modena^{‡*}, Lucia Maini^{†*}

[‡] PolyCrystalLine SPA, Via Della Cooperazione, 29 40059 Medicina, Bologna, Italy

[†] Dipartimento di Chimica "G. Ciamician", via Selmi 2 – Università di Bologna, I-40126, Bologna, Italy

[§] Institut de Ciència de Materials de Barcelona (ICMAB-CSIC), Campus de la UAB, 08193, Bellaterra, Spain

[¤] Laboratory for Chemistry of Novel Materials, University of Mons, 7000 Mons, Belgium

[¥] University of Strasbourg, CNRS, ISIS UMR 7006, 8 Allée Gaspard Monge, Strasbourg, F-67000 France

[¤] Laboratoire de Chimie des Polymères, Faculté des Sciences, Université Libre de Bruxelles (ULB), CP 206/1 Boulevard du Triomphe, 1050, Bruxelles, Belgium

^{¤¤} International Solvay Institutes, Université Libre de Bruxelles (ULB), CP 231 Boulevard du Triomphe, 1050, Bruxelles, Belgium

Table S 1 Solubility test results using 21 different solvents for 5 mg of C7-BTBT-C7 starting material powder. "X": suspension, "YES": clear solution, "-": not performed.

	Temperature	RT (20-25°C)					50°C	75°C
	Volume added to 5 mg	50µL	100µL	250µL	500µL	1mL	1mL	1mL
	Concentration (mg mL ⁻¹)	100	50	20	10	5	5	5
2MX	2-Methoxyethanol	X	X	X	X	X	X	X
2PR	2-Propanol	X	X	X	X	X	X	Yes
ABZ	Benzyl Alcohol	X	X	X	X	X	Yes	-
ACN	Acetonitrile	X	X	X	X	X	X	X
ANI	Anisole	X	Yes	-	-	-	-	-
CHF	Chloroform	Yes	-	-	-	-	-	-
CLB	Chlorobenzene	Yes	-	-	-	-	-	-
DCM	Dichloromethane	Yes	-	-	-	-	-	-
DEC	Diethyl Carbonate	X	X	X	X	Yes	-	-
DMA	N,N-dimethylacetamide	X	X	X	X	X	Yes	-
DMF	N,N-dimethylformamide	X	X	X	X	X	Yes	-
DMS	Dimethyl Sulfoxide	X	X	X	X	X	X	X
DMX	1,2-Dimethoxyethane	X	X	Yes	-	-	-	-
ETH	Ethanol	X	X	X	X	X	X	Yes
H2O	Water	X	X	X	X	X	X	X
IPA	Isopropyl Acetate	X	X	X	X	Yes	-	-
IPE	Isopropyl Ether	X	X	X	Yes	-	-	-
MEK	Methyl ethyl Ketone	X	X	X	Yes	-	-	-
MPY	1-Methyl-2-Pyrrolidone	X	X	X	X	Yes	-	-
PXY	p-Xylene	Yes	-	-	-	-	-	-
THF	Tetrahydrofuran	Yes	-	-	-	-	-	-
TOL	Toluene	Yes	-	-	-	-	-	-

Table S 2 Crystallographic parameters of C7-BTBT-C7 from SCXRD.

Parameters	C7-BTBT-C7
Formula	C ₂₈ H ₃₆ S ₂
Molecular weight (g.mol⁻¹)	218.34
Temperature (K)	293 (2)
Crystal system	Monoclinic
Space group	P 2 ₁ /c
a (Å)	27.260(6)
b (Å)	7.9879(9)
c (Å)	5.9104(6)
β (°)	92.662(16)
V (Å³)	1285.59
Z/Z'	2/0.5
Density (g·cm⁻³)	1.128
F (000)	472
μ (mm⁻¹)	0.219
GOF on F²	1.037
R₁ (on F, I>2σ(I))/R_{ex}	0.0819
WR₂ (F² all data) R_{wp}	0.1525
CCDC number	2225078

Table S 3 Structural and packing descriptors for BTBT cores of C7-BTBT-C7, C8-BTBT-C8 and C12-BTBT-C12

Descriptors	C7	C8	C12
	P2 ₁ /c		
	Monoclinic		
a (Å)	27.26(6)	29.18(4)	37.91(3)
b (Å)	7.988(9)	7.88(1)	7.74(7)
c (Å)	5.910(6)	5.927(7)	5.86(5)
α (°)	90	90	90
β (°)	92.66(16)	92.44(4)	90.59(3)
γ (°)	90	90	90
V (Å³)	1285.60(4)	1361.61	1721.00(3)
Z/Z'	2/0.5	2/0.5	2/0.5
HB (°)	56.48	54.85	53.86
Stacking vector, SV (Å)	5.91	5.93	5.86
Interplanar distance, d(Å)	2.84	2.79	2.71
X (°)	88.52	88.58	88.45
Ψ (°)	28.19	27.38	26.88
Δx	0.15	0.15	0.16
Δy	5.21	5.27	5.23

Pitch (°)	3.08	3.02	3.35
Roll angle (°)	61.40	62.10	62.61
Core tilt angle (°)	87.66	87.87	87.9

Table S 4 Ionization energy (IE) values of C7-BTBT-C7 and other BTBT compounds that are structurally similar as determined by PYS from powder samples.

Compound	IE (eV)
C7-BTBT-C7	5.28 ± 0.02
C8-BTBT-C8	5.33 ± 0.05
C12-BTBT-C12	5.31 ± 0.05

Table S 5 Charge transport parameters and experimental mobilities of C7-, C8- and C12-BTBT.

X-BTBT	J_p (meV)	J_{T1} (meV)	J_{T2} (meV)	λ (meV)	μ_{exp} ($\text{cm}^2/\text{V.s}$)
C7	+51.1	-23.4	-23.4	243.9	1.4
C8	+45.2	-7.1	-7.1	243.6	$1.3^1, 6.2^2, 10^3$
C12	+65.1	-47.2	-47.2	243.1	1.6^4

Table S 6 Electrical characteristics of pristine and PS blended devices of C7-BTBT-C7 with different channel lengths.

Condition	Channel width (μm)	V^{th} Sat (V)	μ_{Sat} ($\text{cm}^2\text{V}^{-1}\text{s}^{-1}$)
Pristine	200	-21.64 ± 0.54	0.19 ± 0.02
	100	-22.46 ± 1.28	0.06 ± 0.00
	50	-23.76 ± 1.85	0.04 ± 0.01
PS10K	200	-31.99 ± 1.45	1.42 ± 0.46
	100	-31.81 ± 1.92	1.28 ± 0.46
	50	-34.22 ± 2.28	0.92 ± 0.03
PS280K	200	-32.78 ± 1.43	0.39 ± 0.09
	100	-36.20 ± 0.57	0.32 ± 0.12
	50	-37.08 ± 0.62	0.25 ± 0.03



Figure S 1 Crystal structure of C7-BTBT-C7. The atomic displacement parameters (ADPs) of carbons in the end of the chain are bigger as there is more degree of freedom in the chains.

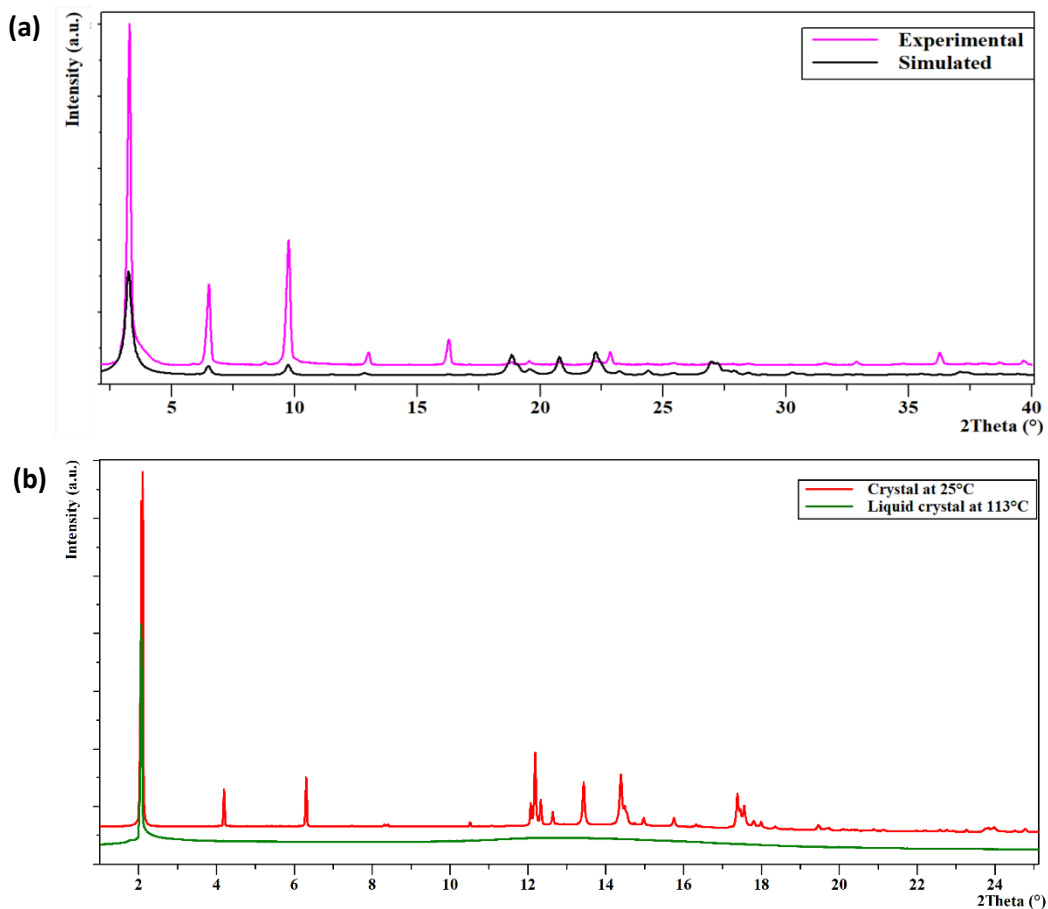
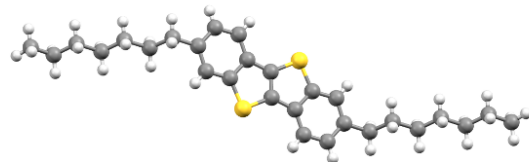


Figure S 2 (a) XRD comparison of simulated (black) and experimental (pink) patterns collected with Bragg-Brentano geometry ($\lambda=1.54 \text{ \AA}$) at 25°C. The real sample dramatically suffers of preferential orientation, and (b) XRD of crystal at 25°C (red) and liquid crystal at 113°C (green) for C7-BTBT-C7 collected with transmission geometry ($\lambda=0.9999613 \text{ \AA}$). In both cases square root scale was used to emphasize the weak peaks.

C7-BTBT-C7



C8-BTBT-C8



C12-BTBT-C12

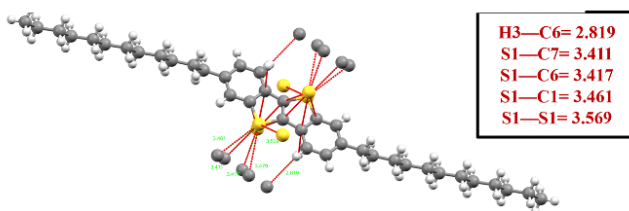
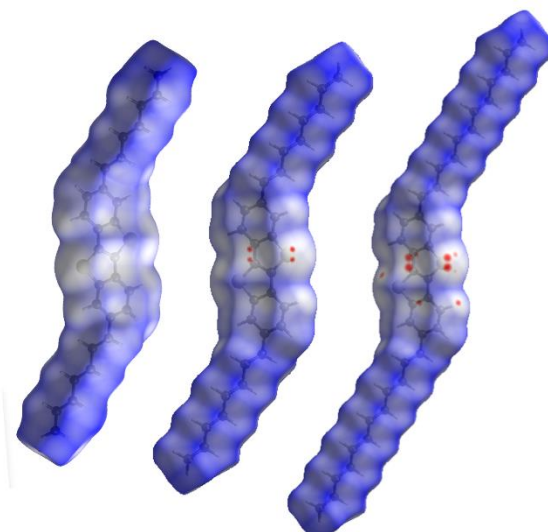


Figure S 3 Short contact interaction in C7-BTBT-C7, C8-BTBT-C8 and C12-BTBT-C12.

(a)



(b)

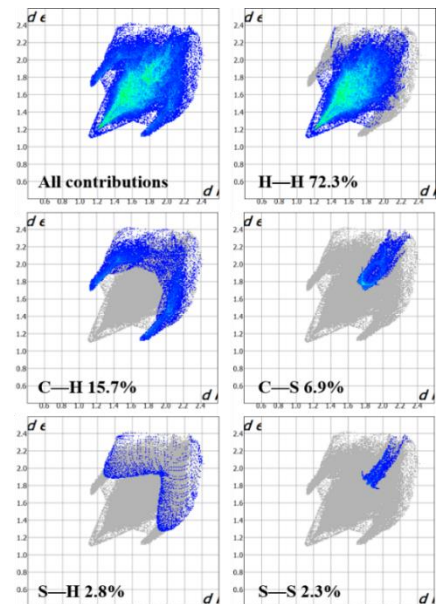


Figure S 4 Hirshfeld surfaces (a) d_{norm} electron density map for C7-BTBT-C7, C8-BTBT-C8 and C12-BTBT-C12 (left to right). Red dots white regions and blue regions are indicative of distances that are shorter, equal, and greater than the van der Waals radii, respectively. (b) 2D fingerprint plots of C7-BTBT-C7 indicating the percentage of contribution of each interaction present in the molecule.

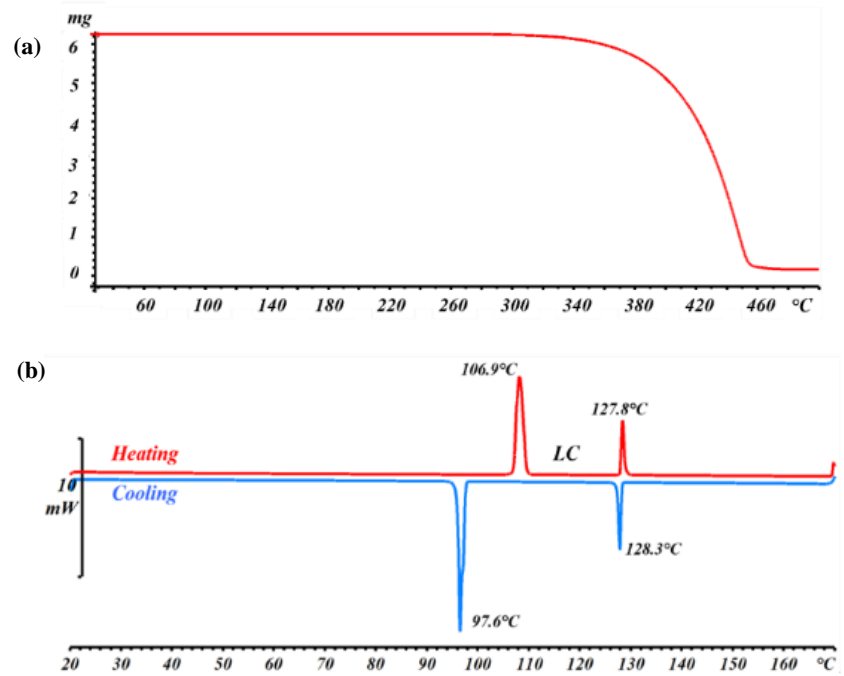


Figure S 5 (a) TGA at a scan rate of $10^{\circ}\text{C min}^{-1}$ and (b) DSC at a scan rate of $5^{\circ}\text{C min}^{-1}$ of C7-BTBT-C7.

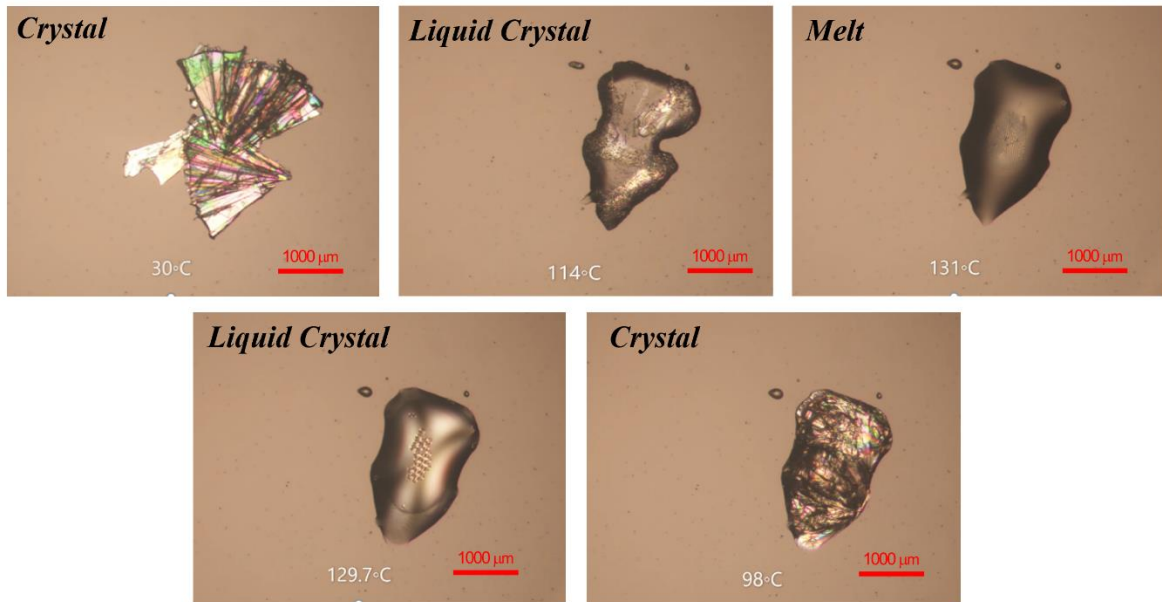


Figure S 6 Hot-stage microscopy images of phase transitions from crystal to liquid crystal, liquid crystal to melt, melt to liquid crystal and liquid crystal to crystal in C7-BTBT-C7. Heating and cooling rates were maintained at $10^{\circ}\text{C min}^{-1}$.

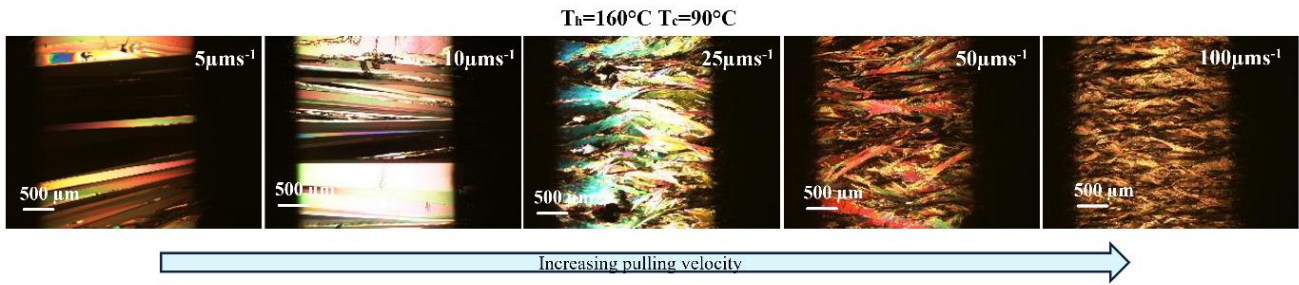


Figure S 7 Polarized optical microscopy images recorded at room temperature after crystallization showing the alignment region with different pulling velocities. The entangled ribbon/needle-like morphology was observed. The entanglement increases with increasing pulling velocity.

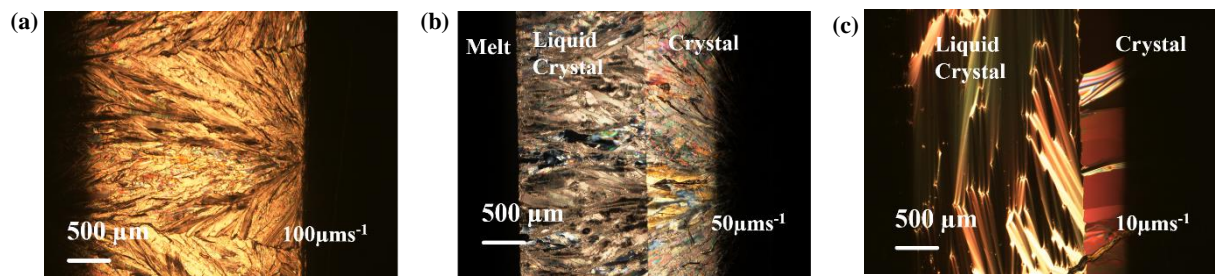


Figure S 8 (a) Multiple nucleation sites (T_h-T_c : 160-90°C) at $100 \mu\text{m s}^{-1}$. (b) Growth Fronts (T_h-T_c : 160-70°C) at $50 \mu\text{m s}^{-1}$. (c) liquid crystal phase was separated by a crystal growth front. The crystal growth front is parallel to the thermal gradient.

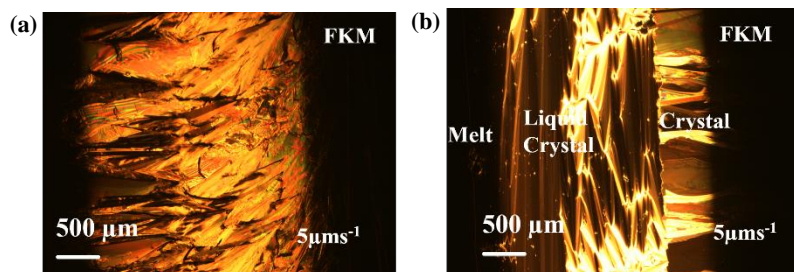


Figure S 9 Polarized optical microscopy images on FKM coated films (pulling velocity $5 \mu\text{m s}^{-1}$) showing (a) nucleation and alignment and (b) growth fronts. The morphology follows the same trend as the films without FKM, and no significant differences in the POM images were observed.

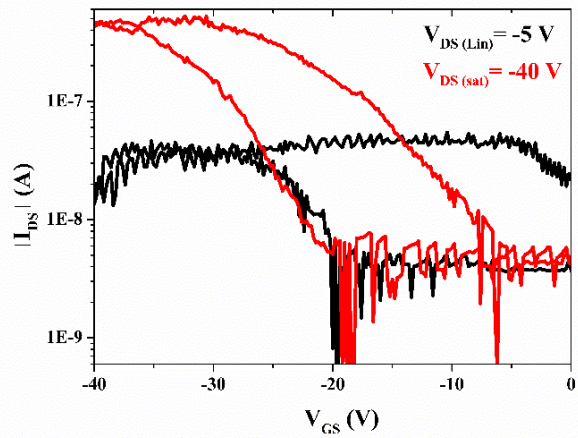


Figure S 10 Representative transfer characteristics showing linear and saturation curves of bottom gate/bottom contact device of C7-BTBT-C7. Channel length 150 μm and channel width/length ratio is 100.

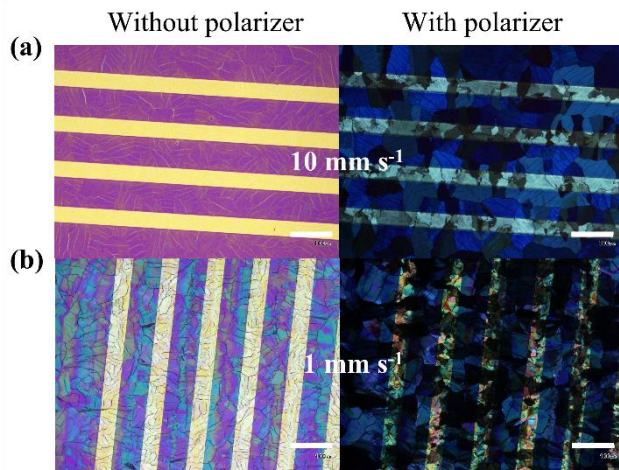


Figure S 11 Polarised optical microscopy (POM) images of bottom gate/bottom contact devices of C7-BTBT-C7 prepared with shearing speed of (a) 10 mm s^{-1} and (b) 1 mm s^{-1} . Scale bar: 200 μm .

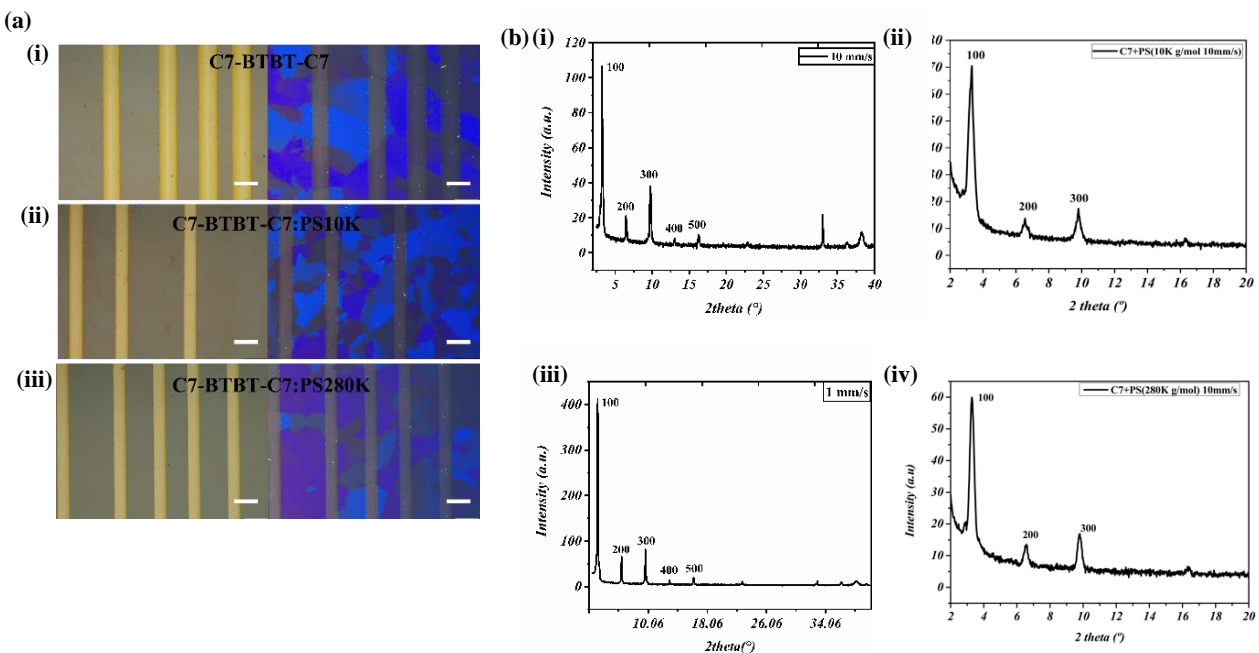


Figure S 12 (a) POM images of bottom gate/top contact devices at 10 mm s^{-1} (i) Pristine (ii) C7-BTBT-C7:PS10K (iii) C7-BTBT-C7:PS280K (The 1 mm s^{-1} films were not homogeneous and did not have full coverage on the electrodes) (b) XRD patterns of (i) Pristine 10 mm s^{-1} (ii) Pristine 1 mm s^{-1} (iii) C7-BTBT-C7:PS10K (10 mm s^{-1}) and (iv) C7-BTBT-C7:PS280K 10 mm s^{-1} . Scale bar: $200 \mu\text{m}$.

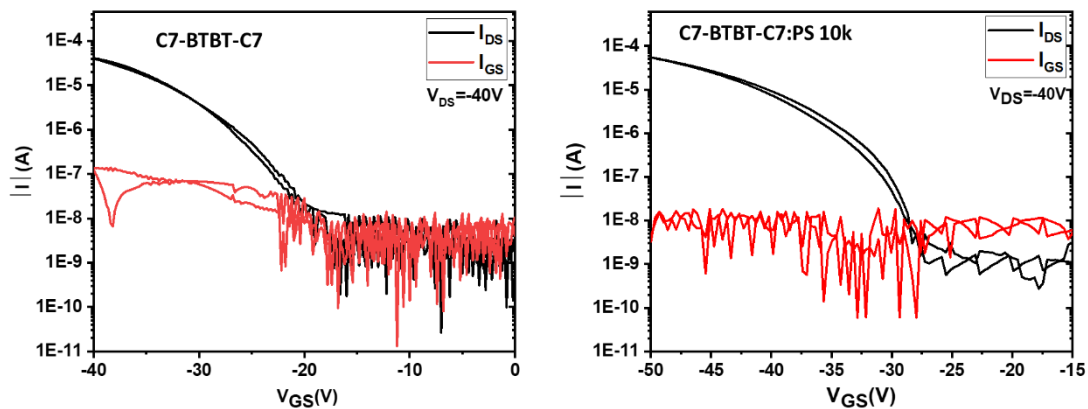


Figure S 13 Transfer characteristics of a representative pristine-based OFET and a blend-based OFET showing the source-gate current (I_{GS}).

References

- 1 J. Li, A. Babuji, I. Temiño, T. Salzillo, F. D'Amico, R. Pfattner, C. Ocal, E. Barrena and M. Mas-Torrent, *Adv Mater Technol*, 2022, **7**, 2101535.
- 2 L. Jiang, J. Liu, X. Lu, L. Fu, Y. Shi, J. Zhang, X. Zhang, H. Geng, Y. Hu, H. Dong, L. Jiang, J. Yu and W. Hu, *J Mater Chem C*, 2018, **6**, 2419–2423.

- 3 R. Janneck, N. Pilet, S. P. Bommanaboyena, B. Watts, P. Heremans, J. Genoe and C. Rolin, *Advanced Materials*, 2017, **29**, 1703864.
- 4 S. Colella, C. Ruzié, G. Schweicher, J.-B. Arlin, J. Karpinska, Y. Geerts and P. Samorì, *Chempluschem*, 2014, **79**, 371–374.